separations

MDPI

Article

Development and Characterization of SBA-15 Imprinted Polymers for Spiramycin Analysis

Lorena González-Gómez [1,2], Sonia Morante-Zarcero [1], Damián Pérez-Quintanilla [1], Gema Paniagua González [2], Rosa M. Garcinuño [2], Pilar Fernández Hernando [2,*] and Isabel Sierra [1,3,*]

[1] Departamento de Tecnología Química y Ambiental, Escuela Superior de Ciencias Experimentales y Tecnología (ESCET), Universidad Rey Juan Carlos, C/Tulipán s/n, Móstoles, 28933 Madrid, Spain; lorena.gonzalez@urjc.es (L.G.-G.); sonia.morante@urjc.es (S.M.-Z.); damian.perez@urjc.es (D.P.-Q.)

[2] Departamento de Ciencias Analíticas, Facultad de Ciencias, Universidad Nacional de Educación a Distancia, Las Rozas, 28232 Madrid, Spain; gpaniagua@ccia.uned.es (G.P.G.)

[3] Instituto de Tecnologías para la Sostenibilidad, Universidad Rey Juan Carlos, C/Tulipán s/n, Móstoles, 28933 Madrid, Spain

* Correspondence: pfhernando@ccia.uned.es (P.F.H.); isabel.sierra@urjc.es (I.S.); Tel.: +34-91-398-72-84 (P.F.H.); +34-91-488-70-18 (I.S.)

Abstract: This work focuses on the development of a hybrid material based on SBA-15 silica with a molecularly imprinted polymer (MIP), using spiramycin (SPI) as a template, for use as sorbent in solid-phase extraction (SPE). Characterization techniques such as nitrogen gas adsorption–desorption isotherms, infrared spectroscopy and scanning electron microscopy confirmed the structure and properties of the SBA-15@MIP-SPI material. SPE conditions using SBA-15@MIP-SPI as sorbent were optimized, which allowed us to demonstrate the high selectivity and adsorption capacity of SPI on the synthesized material. The best conditions were 50 mg of sorbent, loading with 1 mL of standard solution or sample of cow milk previously extracted in acetonitrile and eluting with 3 mL of methanol with 1% acetic acid. After the optimization process, the material demonstrated recovery percentages of 81 ± 3% in SPI standard solutions and showed its potential in cow milk samples (71 ± 6%). The novelty of the research consists of the combination of MIPs with SBA-15, which could offer important advantages in terms of specific surface area and porous structure, thus improving performance and reducing the amount of sorbent compared to other traditional methods.

Keywords: spiramycin; SBA-15; SBA-15@MIP-SPI; hybrid material; molecularly imprinted polymers; solid-phase extraction; SPE; selective material; cow milk

check for updates

Citation: González-Gómez, L.; Morante-Zarcero, S.; Pérez-Quintanilla, D.; González, G.P.; Garcinuño, R.M.; Hernando, P.F.; Sierra, I. Development and Characterization of SBA-15 Imprinted Polymers for Spiramycin Analysis. *Separations* **2024**, *11*, 247. https://doi.org/10.3390/separations11080247

Academic Editor: Antonio Tagarelli

Received: 27 July 2024
Revised: 10 August 2024
Accepted: 13 August 2024
Published: 15 August 2024

Copyright: © 2024 by the authors. Licensee MDPI, Basel, Switzerland. This article is an open access article distributed under the terms and conditions of the Creative Commons Attribution (CC BY) license (https://creativecommons.org/licenses/by/4.0/).

1. Introduction

Spiramycin (SPI) belongs to a group of 16-member macrolide antibiotics and was first obtained from *Streptomyces ambofaciens* in 1954 by Rhône-Poulenc laboratories [1]. The currently known SPI is a mixture of three compounds, SPI I, SPI II and SPI III, with SPI I being the predominant one [2,3]. SPI is metabolized in the organism to neospiramycin, which is identified as the major metabolite [3]. SPI is an antibiotic mainly used around the world because it is effective against several common pathogenic microorganisms, including Gram-positive cocci such as *Staphylococcus aureus*; *Streptococci* of groups A, B, C and D; Gram-negative cocci such as *Neisseria meningitidis* and *Neisseria gonorrhoeae*; protozoa such as *Toxoplasma gondii*; and others [1,4]. In veterinary practice, SPI is employed to treat respiratory diseases in poultry and ruminants, as well as mastitis, arthritis and rinderpest in cattle [4]. The importance of controlling this antibiotic in food is due to its massive use in the meat industry. The growing demand for animal products has increased, with Europe being one of the largest consumers [5]. This increase in production has led to an increased risk of disease spread due to the large number of animals on farms. Consequently, the intensified use of antibiotics such as SPI to treat infections can put consumers' health at risk.

Therefore, the control of such residues in food of animal origin is of paramount importance. The European Union has established maximum residue limits (MRLs) to control such chemical contaminants. Regulation (EU) No 37/2010 [6] sets MRLs for the sum of SPI and neospiramycin between 200 and 300 µg/kg for muscle, fat, liver, kidney and milk of bovine animals; between 200 and 400 µg/kg for muscle, skin, fat and liver of chickens not used for egg production; and for SPI I between 250 and 2000 µg/kg for muscle, liver and kidney of porcine animals.

The matrices in which SPI appears are complex, making it important to include a sample preparation step to eliminate interferences before analysis. SPI analyses are generally carried out by high-performance chromatography (HPLC) with detection systems such as diode array (DAD), ultraviolet (UV), fluorescence (FD), and electrochemical detectors (ECDs) or highly selective detectors, such as mass spectrometry (MS) or tandem mass spectrometry (MS/MS) detectors [7]. The latter are less common in some laboratories as they are an expensive piece of equipment. In the case of HPLC-DAD analyses, it is of great importance to obtain a clean extract free of interferences as they are more prone to be affected by interferents that may hinder the identification of peaks, unlike HPLC-MS or HPLC-MS/MS where the identification of compounds is based on their molecular weight and their fragmentation. SPE is one of the most used techniques in the analysis of antibiotics, including macrolides [7,8], since it allows for the extraction, purification and preconcentration of the analyte, generating clean extracts to inject in HPLC. SPE has been applied with different commercial sorbents for the determination of macrolides in several food samples, such as milk [9–11], eggs [9,11–14] and tissues [9,15]. Generally, the methodologies that apply SPE use commercial cartridges such as Oasis HLB® [9–13] or Bond elut SCX® [15] with large amounts of sorbent, between 200 and 500 mg. These sorbents, besides using large amounts of material, are not specific towards the target analytes, which can be a problem when the analysis is using HPLC-DAD. Moreover, currently, the principles of green analytical chemistry and green sample preparation aim to bring methodologies to miniaturization, consequently reducing the amount of waste [16]. Therefore, the use of new materials such as molecularly imprinted polymers (MIPs) or silica-based materials can be an alternative to commercial materials [17].

MIPs are synthetic materials with predetermined selectivity toward specific target analytes [18,19]. Using molecular imprinting technology, MIPs create recognition cavities that match the size, shape and interactions of template molecules. Once templates are removed, MIPs can selectively rebind to the target molecules [20]. Traditionally, MIPs are prepared through bulk polymerization or precipitation. However, these materials sometimes exhibit certain disadvantages, including reduced binding capacity, challenges in mass transfer and template leakage in the case of conventionally prepared MIPs [21,22].

On the other hand, mesostructured silica materials have aroused great interest within the scientific community and are used in various industrial applications, including catalysis, separation processes and the control of environmental pollution [23]. These materials exhibit a highly ordered mesoporous structure (with pore diameters ranging from 2 to 50 nm according to IUPAC), resulting in well-defined pore sizes, a large pore volume, a high surface area and easily modifiable pores [23–25]. A highly studied mesoporous material is SBA-15-type silica (Santa Barbara Amorphous number 15), developed by Zhao et al. [26], which has a hexagonal structure. This material has great hydrothermal stability due to its thicker, amorphous walls and relatively large pores [23]. Its synthesis is simple; a source of silicon is needed, generally tetraethylorthosilicate (TEOS), a commercial triblock copolymer called Pluronic 123 with amphiphilic character (hydrophilic zone and another hydrophobic zone) and ordering properties, which is used as a director of the structure and acidic conditions with HCl.

For all the above reasons, both materials have gained importance as SPE sorbents. In this sense, hybrid materials that combine mesostructured silicas such as SBA-15 with MIPs can offer a material with highly specific molecular recognition properties, with good extraction performance and a low amount of sorbent [27]. Different investigations that

combine mesostructured silicas with MIPs for the determination of chemical contaminants have been described in the literature as obtaining good extraction yields; for example, Wang et al. [22] used an SBA-15 support with a specific MIP for dicyandiamide, a substance used in fertilizers, applied to the detection of this analyte in milk. Also, some studies used this type of hybrid material for other types of analytes and samples [20,21,28], but now, there is no application of SBA-15-type mesostructured silicas with MIPs used as sorbent in SPE for the determination of SPI in milk samples.

In this work, a hybrid material formed by an MIP within SBA-15-type silica was synthesized and characterized by various techniques. The material was designed as SPE sorbent for the selective determination of SPI in milk samples before its analysis by HPLC-DAD. Different parameters were optimized to assess the selectivity and performance of the synthesized material.

2. Materials and Methods

2.1. Reagents and Materials

Spiramycin (SPI) and five other different types of analytical grade macrolide antibiotics, erythromycin (ERY), roxithromycin (ROX), josamycin (JOS), ivermectin (IVER) and tylosin (TYL), were purchased from Sigma Aldrich (St. Louis, MO, USA). Stock standard solutions (1000 mg/L) of each antibiotic were prepared by diluting 10 mg in 10 mL of acetonitrile (ACN). Standard working solutions were prepared at the desired concentrations in NaH_2PO_4/ACN (70:30, *v*/*v*). All solutions were stored at −20 °C in darkness.

LC-grade solvents such as ACN, methanol (MeOH) and *n*-hexane; synthesis-grade toluene and acetone; HCl (37%, 36.45 g/mol, 1.19 g/mL); acetic acid (HAc 60,052 g/mol, 1.05 g/mL); and NaOH were purchased from Scharlab (Barcelona, Spain). Reagents for synthesis, such as tetraethylorthosilicate (TEOS, 98%, 208.3 g/mol, 0.93 g/mL), poly(ethylene-glycol)-block-poly (propylene-glycol)-block-poly (ethylene-glycol) (EO20PO70EO20, Pluronic 123, 5800 g/mol, 1.019 g/mL), ethylene glycol dimethacrylate (EGDMA), methacrylic acid (MAA), sodium diethyldithiocarbamate (Na-DTC) and tetrahydrofuran (THF), were obtained from Sigma-Aldrich (St. Louis, MO, USA). 4-(chloromethyl)-phenyltrimethoxysilane (CPTS) was acquired from AbcrGmbH (Karlsruhe, Germany). Sodium phosphate monobasic (NaH_2PO_4) used for mobile phase preparation and Scharlab ExtraVac® vacuum manifold (12-port model) used for SPE were obtained from Scharlab (Barcelona, Spain). Polyethylene frits (0.20 µm), empty syringes (3 mL), nylon syringe filters (0.45 µm, 13 mm) and nylon membranes (0.45 µm pore size) were obtained from Mervilab (Madrid, Spain). The Milli-Q water (resistivity 18.2 MΩ cm) used in this work was obtained from a Millipore Milli-Q-System (Billerica, MA, USA).

2.2. Synthesis of SBA-15 and SBA-15@MIP-SPI

2.2.1. Synthesis of SBA-15

The synthesis of SBA-15 followed the procedure described by Zhao et al. [29]. Initially, 19.4 g of Pluronic 123 was dissolved in a mixture of 576 mL of 2 M HCl and 144 mL of H_2O. The dissolution process occurred under stirring at 400 rpm and 35 °C. Subsequently, 40.8 g of TEOS was added dropwise, and the mixture was stirred for 20 h. After this period, the stirring was halted and the temperature was raised to 80 °C for an additional 24 h (aging process). The resulting material was filtered, washed with distilled water to remove the surfactant (P123) and air-dried. Finally, the material was transferred to a porcelain dish and calcined by ramping up the temperature to 500 °C over 8.5 h and then holding it at 500 °C for 12 h.

2.2.2. Preparation of SBA-15@MIP-SPI

In this first step, 2.5 g of SBA-15 was placed in a Schlenk and covered with 25 mL of CPTS solution at 5% (*v*/*v*) in dry toluene with an excess of CPTS (1.4 mL more). The mixture was heated to 55 °C in a liquid silicone bath to maintain the temperature. The synthesis was carried out with stirring (300 rpm) for 42 h, ensuring that the temperature

remained stable throughout. After this time, the obtained material was washed three times with 10 mL of dry toluene and twice with 10 mL of acetone. Finally, it was left to dry for 2 h in the oven at a temperature of 70 °C.

Once the SBA-15 silica was silanized, 0.8 g was weighted and the polymerization initiator, Na-DTC, was fixed. For this purpose, the silanized material was kept for 4 h at 40 °C with 10 mL of 2% (*w*/*v*) Na-DTC solution in THF. After 4 h, the material was washed with 10 mL of THF, Milli-Q water, MeOH and acetone.

Finally, 0.6 g of the silanized material and the initiator were put in contact with 32 mg of SPI (template molecule), 350 µL of the functional monomer, MAA, and 3772 µL of crosslinking monomer, EGDMA, and were added to 14 mL of the porogen solvent, ACN. The molar ratio of the template molecule/functional monomer/cross-linker was 1:2:10. The polymerization of the mixture was carried out under UV irradiation for 6 h at 365 nm, always maintaining a nitrogen atmosphere. This process was carried out twice to ensure polymerization. To obtain the NIP, the same process was carried out, but without adding SPI to the polymeric mixture. Figure 1 summarizes this process.

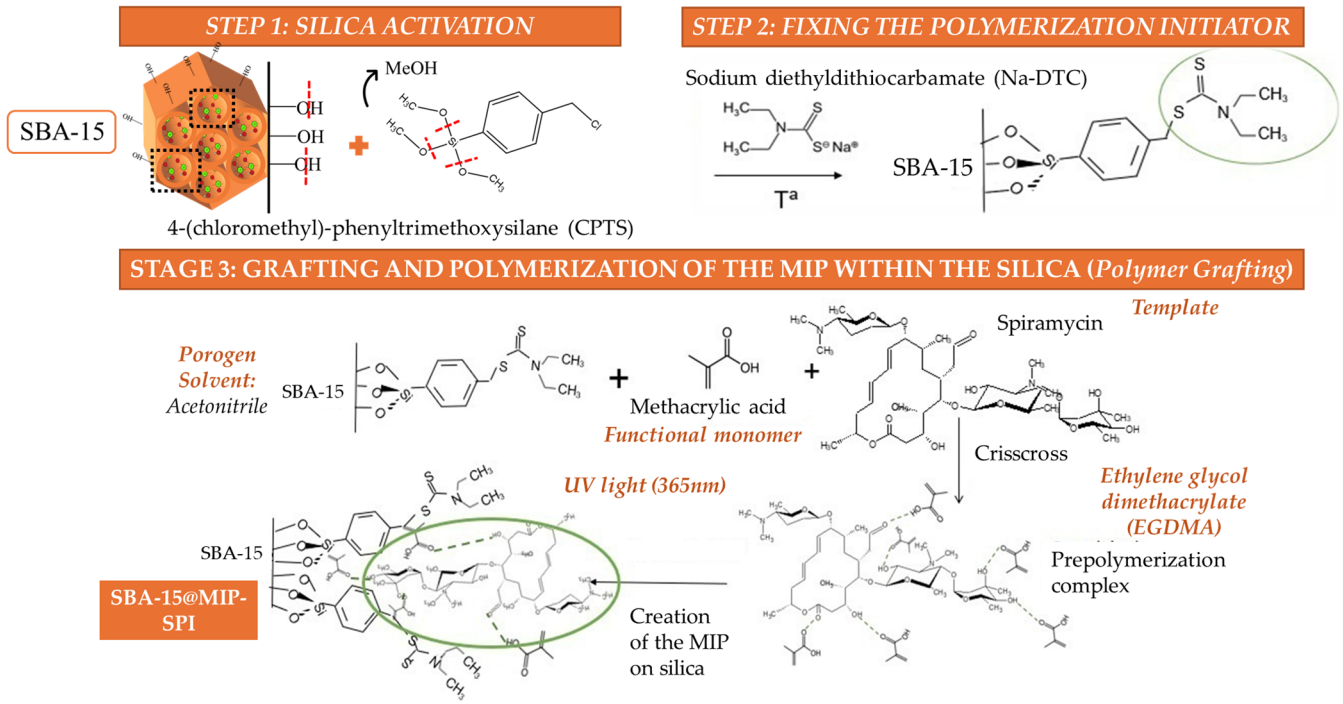


Figure 1. Synthesis of MIP within SBA-15-type silica.

After completing these three steps, the template molecule was extracted using two methods, orbital shaker extraction (1 h at 60 °C and 130 rpm, with 20 mL volumes of 0.5% (*v*/*v*) acetic acid in MeOH) and then Soxhlet extraction (6 h, with volumes of 80 mL of 0.5% (*v*/*v*) acetic acid in MeOH), as the previous technique was not sufficient to completely remove the template. As Soxhlet extraction was found to be a more efficient technique for template extraction, in the following batches' synthesis, only Soxhlet extraction for 12 h was used.

2.3. Characterization of the Synthesized Material

The SBA-15 silica, SBA-15@MIP-SPI and SBA-15@NIP were characterized using nitrogen gas adsorption–desorption isotherms, scanning electron microscopy (SEM) and attenuated total reflection Fourier transform infrared spectroscopy (ATR-FT-IR). The surface-specific area (S_{BET}) was determined by recording N_2 gas adsorption–desorption isotherms using a Micromeritics ASAP 2020 analyzer. Additionally, the pore size distribution was obtained from the desorption branch using the Barrett–Joyner–Halenda (BJH) model. Before

conducting the analysis, the materials underwent overnight drying in a vacuum line and subsequent degassing at 90 °C under vacuum for 10 h in the porosimeter's degassing port. The nitrogen adsorption–desorption data were then recorded at a temperature of −196 °C using liquid nitrogen. The surface morphology of the studied materials was examined using an EM-30AX Plus COXEM microscope from JASCO (COXEM Co, Daejeon, Republic of Korea) for SEM. Before conducting the analysis, the samples underwent Au coating using an SPT-20 sputter coater. The materials were positioned in a metal stub with the help of a sticky carbon disk, and they were subsequently coated with a 50 nm layer of gold (applied for 300 s at 50 mA). Finally, the samples were observed at an accelerated voltage of 20 kV, with magnification ranging from 70 to 100,000 times. Identification of the main functional groups was performed by recording ATR-FT-IR spectra using a Jasco FT-IR 4100 (Jasco, Tokyo, Japan) in the wavelength range of 4000–450 cm^{-1}.

2.4. Solid-Phase Extraction Conditions

Empty cartridges were packed with 50 mg of SBA-15@MIP-SPI or SBA-15@NIP material and plugged with polyethylene frits at both ends. A nylon membrane (0.45 µm pore size) was also inserted at the bottom of the sorbent bed to prevent material loss during sample loading. The cartridges with the packed material were conditioned with 1 × 3 mL of ACN, followed by 1 mL of a solution of 5 µg/mL SPI in ACN. This was followed by a washing step with hexane (1 × 2 mL) and, finally, the analyte was eluted with 1 × 3 mL of MeOH with 1% acetic acid (Figure 2). Eluates were evaporated to dryness with a stream of nitrogen and redissolved with 300 µL of NaH_2PO_4/ACN (70:30, *v*/*v*) for HPLC-DAD determination (see Section 2.5).

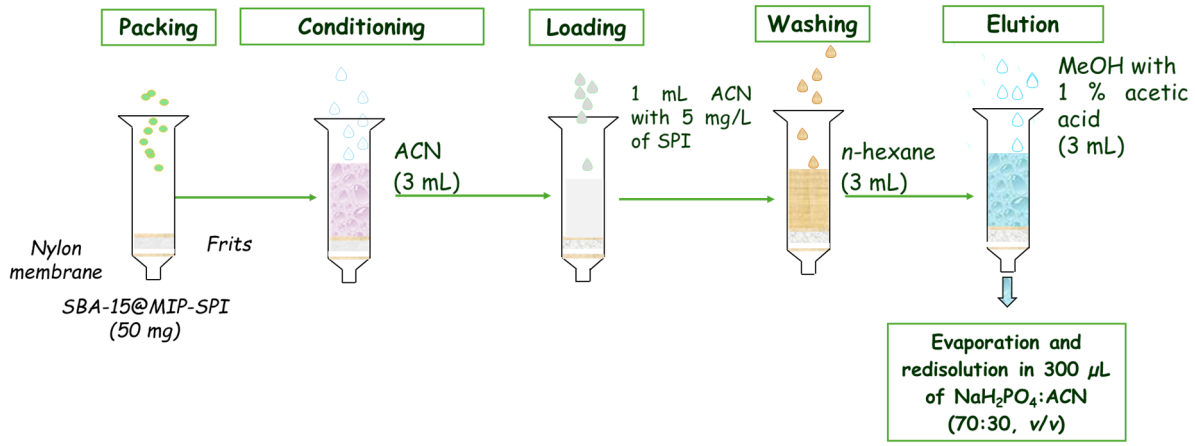


Figure 2. Solid-phase extraction conditions and steps using SBA-15@MIP-SPI.

2.5. Chromatographic Conditions

An Agilent 1200 series Liquid Chromatography system (Agilent Technologies, Waldbronn, Germany), with an Agilent 1290 quaternary pump, an autosampler with a 20 µL loop, a thermostated column compartment and a photo-diode array detector, was used to evaluate the performance of the synthesized material. The instrumental parameters were controlled via the Agilent ChemStation software Rev. B. 04. 02. 96. The analytical column used for the separation was a Prontosil Hypersorb ODS (5.0 µm, 250 × 4.6 mm, Scharlab, Barcelona, Spain). The injection volume was 20 µL, and the temperature of the column throughout the analysis was maintained at 60 °C. The separation was in gradient, combining solvent A (ACN) and solvent B (phosphate-buffer solution, 25 mM, pH 7). The phosphate-buffer solution was prepared by dissolving the appropriate amount of NaH_2PO_4 in Milli-Q water and adjusting the pH with NaOH solution (5 M) to pH 7. The total runtime was 20 min. The gradient program is shown in Table 1.

Table 1. Gradient program for analytical determination of SPI.

Time (min)	% ACN	% Phosphate Buffer	Flow (mL/min)
0	50	50	1.000
3	50	50	1.000
7	58	42	1.200
15	58	42	1.200
16	70	30	1.500
20	70	30	1.500

SPI quantification was performed using peak area measurements at a wavelength of 231 nm.

2.6. Sample Preparation

To assess the usefulness of the synthesized material, it was applied to milk samples. The semi-skimmed cow milk samples were purchased from local supermarkets in Madrid, Spain. The samples were doped with SPI at a concentration of 5 µg/mL. After doping, the samples were stabilized at room temperature for 20 min. Then, 1 mL was collected and subjected to a deproteinization process with 4 mL of ACN. The samples were centrifuged for 10 min at 2500 rpm and filtered with a 0.45 µm nylon filter. Subsequently, the optimized process described in Section 2.4 was carried out.

3. Results and Discussion

3.1. Characterization of the SBA-15 and SBA-15@MIP-SPI

3.1.1. Textural Characterization of Materials Synthesized through Nitrogen Physisorption

The textural characterization of the materials was carried out by nitrogen physisorption. Through this analysis, the pore size distribution, surface area and pore volume of the synthesized materials were determined. Table 2 summarizes the data obtained after nitrogen physisorption analysis. This analysis showed that after the formation of the hybrid material the pore diameter decreased considerably, from 56 to 35 Å (Table 2, Figure 3a). This was caused by the formation of the polymer on the surface of the silica pore, which caused the pore diameter to decrease concerning the starting material (SBA-15). The surface area and pore volume were also seen to decrease due to the presence of MIP (Table 2). On the other hand, Figure 3a not only shows a decrease in the pore diameter after the formation of the MIP, but the grafted MIP has good homogeneity.

Table 2. Textural properties of synthesized materials.

Silica	S_{BET} [a] (m^2/g)	BJH Pore Diameter [b] (Å)	Pore Volume [c] (cm^3/g)
SBA-15	998.5	56.0	1.02
SBA-15@MIP-SPI	404.9	35.1	0.33

[a] S_{BET}: specific surface area calculated by Brunauer–Emmett–Teller (BET) method. [b] BJH pore diameter: estimated by Barrett–Joyner–Halenda (BJH) model applied in the desorption branch. [c] Pore volume: total pore volume measured at relative $P/P_0 = 0.97$.

As for the N_2 adsorption–desorption isotherms (Figure 3b,c), they show a type IV isotherm, according to the IUPAC classification, with a hysteresis cycle typical of mesoporous materials. The formation of this hysteresis cycle (H_1) in the SBA-15 and SBA-15@MIP-SPI represents the capillary condensation of nitrogen within the uniform mesoporous structure. The condensation of the synthesized material occurs at intermediate relative pressures typical of materials with a normal pore size, such as that of the materials studied.

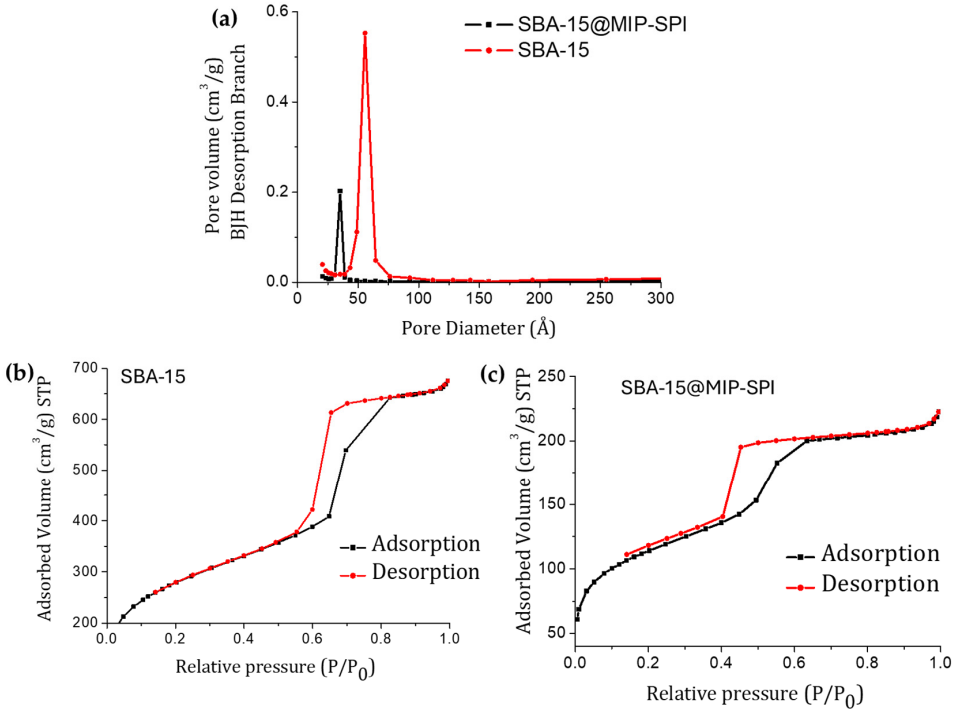


Figure 3. Pore size distribution of (**a**) SBA-15 in comparison with SBA-15@MIP-SPI and nitrogen adsorption–desorption isotherms of (**b**) SBA-15 and (**c**) SBA-15@MIP-SPI.

3.1.2. FT-IR Spectra

ATR-FT-IR spectra are shown in Figure 4. A broad band is observed at 1062 cm^{-1}, attributed to the siloxane groups (Si-O-Si). This band is associated with typical asymmetric stretching, as can be seen in the spectrum shown in Figure 4. Other typical bands found are the vibration of Si-OH at 956 cm^{-1}, the symmetric stretching of the Si-O bond of the siloxane groups around 800 cm^{-1} and a bending of Si-O-Si at 438 cm^{-1}, all characteristic of mesoporous silicas. On the other hand, the SBA-15@MIP-SPI is characterized by a band corresponding to a stretching of a carbonyl group, C=O, at 1721 cm^{-1}, characteristic of methacrylic acid, confirming the correct formation of the MIP. Also, adsorption bands were found at 1627 cm^{-1} and 3325 cm^{-1} caused by irregular vibrations, OH stretching or the bending vibrations of adsorbed water molecules. The absorption peak at 2344 cm^{-1} corresponds to the asymmetric stretching vibration of atmospheric carbon dioxide.

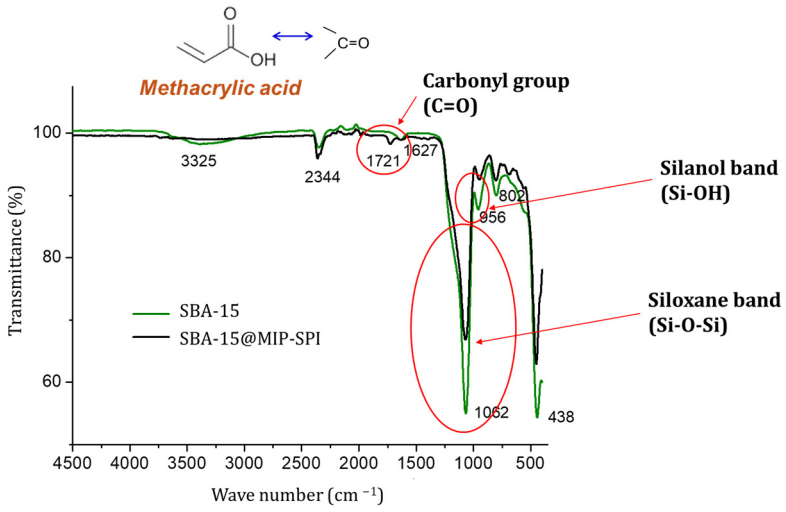


Figure 4. ATR-FT-IR spectra of SBA-15 and SBA-15@MIP-SPI.

3.1.3. Morphological Study by SEM

The morphology of the materials synthesized in this work (SBA-15, SBA-15@MIP-SPI and SBA-15@NIP) was studied using an SEM; images of the three materials are shown in Figure 5. As can be seen in Figure 5A,B, the particles of the SBA-15-type silica are quasi-spherical in shape, with particle diameters varying between 200 and 500 nm. In contrast, the SBA-15@MIP-SPI material has fewer spherical and bulky particles than SBA-15 (Figure 5C). These differences in size and shape indicate that the surface of this material was surface-printed. SEM analysis was also performed on the unprinted material (SBA-15@NIP), synthesized with the same process as SBA-15@MIP-SPI but without the addition of SPI in the polymeric mixture. The SEM result of the SBA-15@NIP material shows more agglomerated and undefined particles, unlike SBA-15@MIP-SPI, indicating that the MIP correctly formed on the outer surface of the silica.

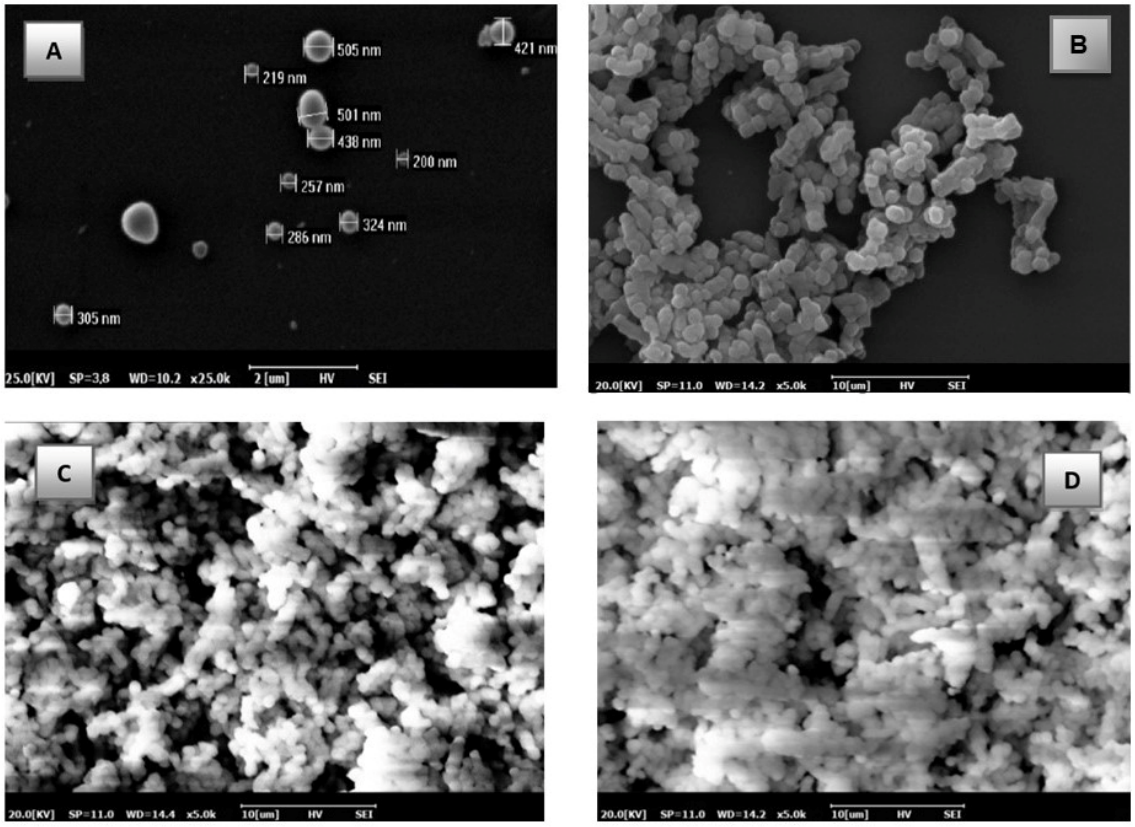


Figure 5. SEM images of (**A**) SBA-15 at × 25.0 K, (**B**) SBA-15 at ×5.0 K, (**C**) SBA-15@MIP-SPI at × 5.0 K and (**D**) SBA-15@NIP at × 5.0 K.

3.2. Assessment of the SBA-15@MIP-SPI as SPE Sorbent

In this study, different studies were carried out to evaluate the extraction capacity and selectivity of the prepared hybrid material and optimize the experimental conditions that affect the recognition of the SPI antibiotic by the SBA-15@MIP-SPI material during the SPE process. SPE consists of conditioning, loading, washing and elution, so each stage of this process was evaluated for maximum performance. Thereupon, parameters such as flow rate, loading, washing and elution solvent were optimized.

To start the optimization, 50 mg of the synthesized material was packaged to miniaturize the method, since below 100 mg the SPE can be considered miniaturized [30]. Following this step, the loading solvent was checked. For this test, ACN and mixtures of ACN with water in 90:10, 70:30 and 50:50 (v/v) ratios were selected. ACN was selected because, being the porogen in the synthesis process, it can favor specific interactions between the functional groups of the analyte and the functional monomer. For this test, different standard

SPI solutions at a concentration of 5 µg/mL prepared in the solvents described above were used and 1 mL of these solutions was loaded into the cartridge previously conditioned with 1 × 3 mL of the same loading solvent. The flow in this experiment was set at 0.1 mL/min. The eluate obtained from the loading step was evaporated, reconstituted in 300 µL of NaH_2PO_4/ACN (70:30, *v*/*v*) and injected into HPLC-DAD. The obtained area was interpolated on an external standard calibration curve (0.1–15 µg/mL) to obtain the concentrations and to calculate the percentage recovery (%). The following formula was used to calculate the percentage recovery: % = (concentration of SPI recovered after purification/concentration of SPI originally taken) × 100. Figure 6 shows the results obtained from this test. As can be seen in Figure 6, ACN demonstrated only 2% recovery, which indicates that SPI was completely retained in the sorbent, unlike the rest of the solvents in which SPI was recovered between 44 and 77%. Mixtures of ACN with water seem to not allow interactions of the analyte with the material. Therefore, ACN was selected as the loading solvent to evaluate the rest of the steps. Next, the test was repeated, increasing the flow to 0.2 mL/min to accelerate the process. The results showed that by increasing the flow, the recovery percentage in the loading stage increased from 2 ± 2% to 33 ± 3%. This result showed that a higher flow makes the interaction between the target analyte and the sorbent more difficult. Therefore, 0.1 mL/min was set as the flow for the rest of the experiments.

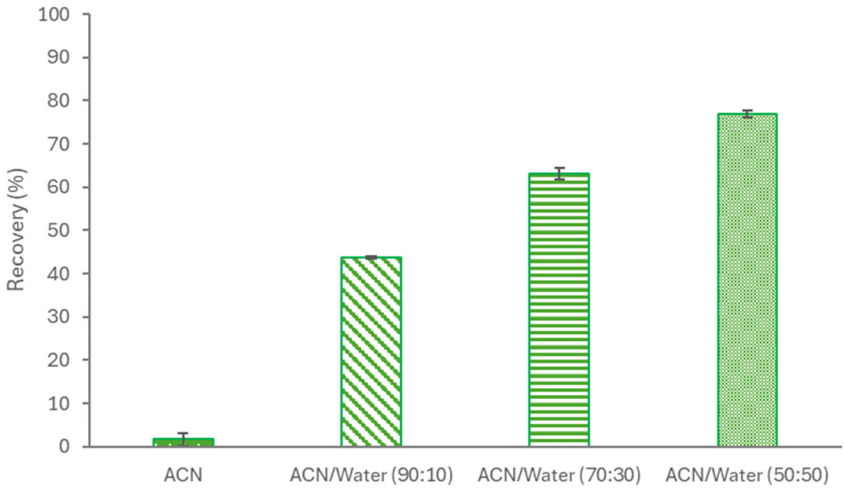


Figure 6. Effect of the loading solvent on the recovery (%) of SPI in the SBA-15@MIP-SPI.

The next stage to optimize was the washing stage. This step is important to eliminate non-specific interactions with interfering molecules that the samples may contain. Therefore, it is important to select a solvent that eliminates these interferents without affecting the interaction of the analyte of interest. In this stage, 1 × 2 mL of ACN, methanol or hexane were tested. This experiment was carried out with standard solutions as described above. The best results were obtained with hexane since no SPI peak was observed in the chromatogram (0% recovery). This solvent is not capable of breaking the interactions of SPI with SBA-15@MIP-SPI, but it can be very useful for removing fat when a milk sample is purified in this sorbent. The other solvents tested as washing solvents showed recovery percentages of 31 ± 1% for MeOH and 4.6 ± 0.6% for ACN, so hexane was set as a washing solvent.

Finally, the effect of the solvent on the elution was evaluated. For this, the previously optimized parameters were used. The cartridge was conditioned with ACN (1 × 3 mL), 1 × 1 mL of standard solution in ACN was loaded, the cartridge was washed with 1 × 3 mL of hexane and different elution solvents were tested: mixtures of methanol water and methanol with acid up to 1%. Percentages greater than 1% of HAc were not tested, because previous studies [31] demonstrated the instability of SPI in more acidic media. Figure 7 demonstrates that the best recovery percentages were obtained with MeOH with 1% HAc.

This small amount of acid seems to break the analyte–sorbent interactions, so this solvent was selected to complete the optimization of the SPE process.

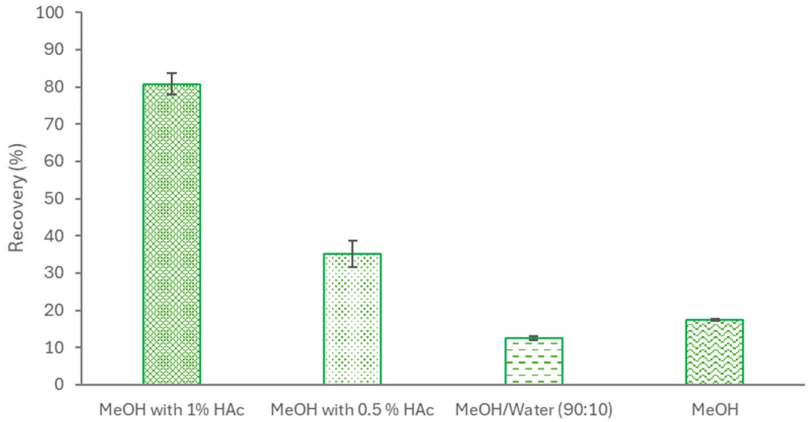


Figure 7. Effect of elution solvent on SPI recovery in SBA-15@MIP-SPI.

3.3. Selectivity of SBA-15@MIP-SPI vs. SBA-15@NIP

With the conditions obtained in Section 3.2, the selectivity and the effect of printing of SBA-15@MIP-SPI versus SBA-15@NIP were checked. Figure 8 shows how the SBA-15@MIP-SPI material is capable of retaining and eluting the SPI completely (86 ± 1%), unlike SBA-15@NIP (19 ± 3), which loses around 40% of the SPI during loading and is only capable of eluting around 19%. This fact demonstrates the superior selectivity of SBA-15@MIP-SPI against SPI compared to SBA-15@NIP, demonstrating that it is a highly selective and effective sorbent for the extraction and purification of SPI.

On the other hand, a test was carried out with other macrolides (ERY, JOS, ROX and TYL) and SPI. For this test, the optimized conditions in Section 3.2 were used, but in this case, 1 mL of a solution containing 5 ppm of SPI, JOS, ROX, IVER, ERY and TYL was used. Both synthesized materials, SBA-15@MIP-SPI and SBA-15@NIP, were compared with each other. The results obtained are shown in Figure 9. From this test using SBA-15@MIP-SPI, recoveries between 0 and 35% for JOS, ROX, IVER, ERY and TYL and around 83% for SPI were seen, demonstrating that this material is only selective to SPI. In the case of the SBA-15-NIP material, the results were poor for all the analytes studied with recoveries between 0 and 21%, being in SPI 14 ± 2%.

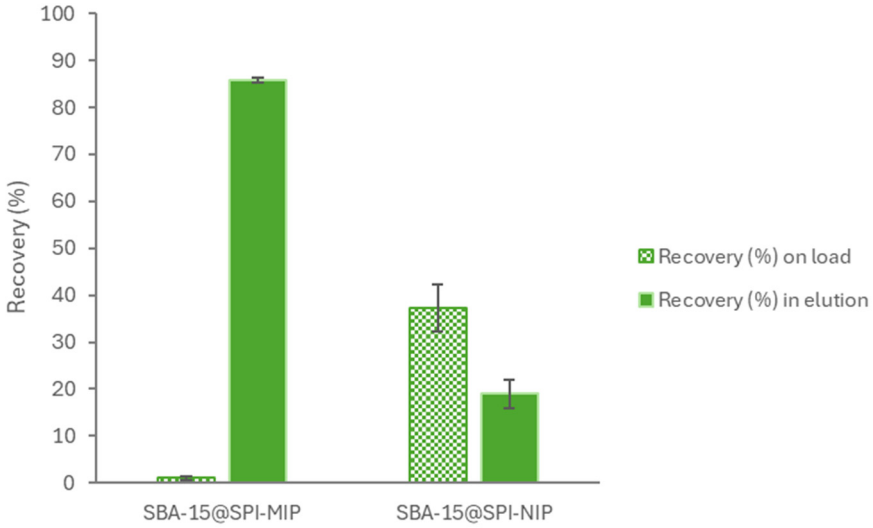


Figure 8. Comparison of SBA-15@MIP-SPI and SBA-15@NIP during loading and elution of SPI (5 µg/mL) in SPE.

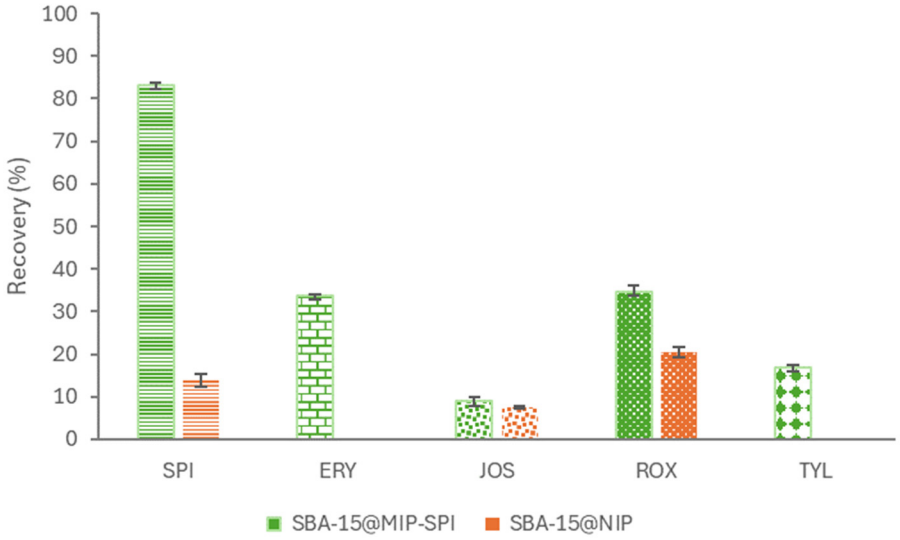


Figure 9. Comparison of SBA-15@MIP-SPI and SBA-15@NIP during loading and elution of 5 different type of macrolides (5 µg/mL), SPI, ERY, JOS, ROX and TYL, in SPE.

3.4. Performance of the Method

Instrumental linearity was evaluated using SPI standard solutions in NaH_2PO_4/ACN (70:30, *v*/*v*). Seven points were prepared in the range of 0.1 to 15 µg/mL from the stock standard solutions of SPI. The slope and intercept of the calibration curve for SPI were determined through regression analysis. A linear relationship was observed between the corrected peak areas and the analyte concentration, with a regression coefficient (R^2) equal to 0.999 (Table 3). The instrumental detection limits (LODs) and quantification limits (LOQs) were calculated with a signal-to-noise ratio of 3 and 10 in the solution at the lowest injected concentration (0.1 µg/mL). The LOD and LOQ obtained were 0.01 µg/mL and 0.04 µg/mL, respectively. The limit of quantification (MQL) and detection limit (MDL) of the method were calculated with a signal-to-noise ratio of 3 and 10 using spiked samples considering the entire protocol. The MQL in the milk sample was 0.028 µg/g and the MDL was 0.008 µg/g. These limits are similar to those obtained by other authors such as García et al. [31] (0.024 µg/g) and show the high sensitivity of the method. The accuracy and precision of the method using SBA-15@MIP-SPI as sorbent was tested in triplicate using standard solutions at a concentration of 5 µg/mL and the optimized conditions (see Section 2.4). The recovery percentage (%) calculated for accuracy was acceptable, specifically 81 ± 3% (Table 3). On the other hand, intra-day (*n* = 3, 1 day) and inter-day (*n* = 3, 3 days) precision was evaluated, demonstrating a low RSD % < 5% in both studies (Table 3).

Table 3. Methodology performance results.

Linear Range (µg/mL)	Linearity R^2	LOD [a] MDL (µg/mL or µg/g)	LOQ [b] MQL (µg/mL or µg/g)	Accuracy *n* = 3 (Recovery ± SD %)	Intra-Day Precision *n* = 3, 1 day (RSD %)	Inter-Day Precision *n* = 3, 3 days (RSD %)
0.1–15	25.15× + 0.84 0.999	0.01 0.008	0.04 0.028	81 ± 3	0.6	4.4

[a] LOD or MDL: limit of detection or method quantification limit. [b] LOQ or MQL: limit of quantification or method detection limit.

3.5. Application of SBA-15@MIP-SPI in SPI-Spiked Milk Samples

To demonstrate the good performance of the synthesized material (SBA-15@MIP-SPI) and its applicability, it was tested with the optimized conditions but with loading with 1 mL of previously deproteinized doped milk, as indicated in Section 2.6. Simultaneously and with the same conditions, the same test was carried out with SBA-15@NIP. The recovery

percentages were 71 ± 6% for the SBA-15@MIP-SPI material and 14 ± 6% for SBA-15@NIP, demonstrating acceptable results on the sample for the SBA-15@MIP-SPI.

3.6. Comparison with Other Methodologies

Our analytical methodology using SBA-15@MIP-SPI represents a significant advancement in SPE for the determination of SPI. The innovative use of SBA-15 with a MIP specific to SPI not only enhances the selectivity and sensitivity of the extraction process but also markedly reduces the quantity of sorbent required. This improvement can be demonstrated if it is compared with the methodology of García et al. [31], which offers very good results but uses 200 mg of MIP. The SBA-15@MIP-SPI leverages the high surface area and tailored pore structure of SBA-15, which, when combined with SPI-specific imprinting, achieves superior adsorption capacity and efficiency. This enables a substantial decrease in the amount of sorbent material required, maintaining extraction performance and making the method more cost-effective compared to conventional MIP.

4. Conclusions

In this work, a material was prepared by combining SBA-15-type mesostructured silicas with MIPs for the selective extraction of SPI from milk samples. The characterization techniques used (nitrogen physisorption, SEM and FTIR) demonstrated the success of the synthesis of SBA-15@MIP-SPI with respect to SBA-15@NIP and allowed us to confirm the structure and properties of the synthesized material.

The optimization experiments demonstrated good performance of the material applied as SPE sorbent and high selectivity towards SPI with better recoveries of SBA-15@MIP-SPI (86 ± 1%) concerning SBA-15@NIP (19 ± 3%) and with respect to other antibiotics of the macrolide family. The material demonstrated good performance, demonstrating adequate precision and accuracy. It was also successfully applied to milk samples, demonstrating its applicability. This study demonstrates that MIPs combined with SBA-15 are highly efficient in the extraction of specific compounds from food matrices.

Author Contributions: Conceptualization, P.F.H., I.S., R.M.G.; methodology, R.M.G., S.M.-Z.; software, L.G.-G.; validation, L.G.-G.; formal analysis, L.G.-G.; investigation, L.G-G., D.P.-Q., G.P.G.; resources, L.G.-G.; data curation, L.G.-G.; writing—original draft preparation, L.G.-G.; writing—review and editing, L.G.-G., D.P.-Q., S.M.-Z., R.M.G., P.F.H., I.S; visualization, S.M.-Z.; supervision, R.M.G., D.P.-Q., G.P.G.; project administration, P.F.H., I.S.; funding acquisition, P.F.H., I.S. All authors have read and agreed to the published version of the manuscript.

Funding: This work was supported by the Comunidad of Madrid and European funding from the FSE and FEDER programs (project S2018/BAA-4393, AVANSECAL-II-CM).

Data Availability Statement: Data is contained within the article.

Conflicts of Interest: The authors declare no conflicts of interest.

References

1. Chabbert, Y.A. Early studies on in-vitro and experimental activity of spiramycin: A review. *J. Antimicrob. Chemother.* **1988**, *22*, 1–11. [CrossRef] [PubMed]
2. Kanfer, I.; Skinner, M.F.; Walker, R.B. Analysis of macrolide antibiotics. *J. Chromatogr. A* **1998**, *812*, 255–286. [CrossRef] [PubMed]
3. Wang, J.; Leung, D. Determination of spiramycin and neospiramycin antibiotic residues in raw milk using LC/ESI-MS/MS and solid-phase extraction. *J. Sep. Sci.* **2009**, *32*, 681–688. [CrossRef] [PubMed]
4. Elazab, S.T.; Elshater, N.S.; Hashem, Y.H.; Al-Atfeehy, N.M.; Lee, E.B.; Park, S.C.; Hsu, W.H. Pharmacokinetic/pharmacodynamic modeling of spiramycin against mycoplasma synoviae in chickens. *Pathogens* **2021**, *10*, 1238. [CrossRef] [PubMed]
5. Henchion, M.; Moloney, A.P.; Hyland, J.; Zimmermann, J.; McCarthy, S. Review: Trends for meat, milk and egg consumption for the next decades and the role played by livestock systems in the global production of proteins. *Animal* **2021**, *15*, 100287. [CrossRef] [PubMed]
6. Commission Regulation (EU) No 37/2010 of 22 December 2009 on Pharmacologically Active Substances and Their Classification Regarding in Foodstuffs of Animal Origin Maximum Residue Limits in Foodstuffs of Animal Origin. *Off. J. Eur. Union*. Available online: https://health.ec.europa.eu/system/files/2016-11/reg_2010_37_en_0.pdf (accessed on 5 September 2023).

7. Hu, C.; Zhang, Y.; Zhou, Y.; Liu, Z.; Meng, Q.; Feng, X. song A review of pretreatment and analysis of macrolides in food (Update Since 2010). *J. Chromatogr. A* **2020**, *1634*, 461662. [CrossRef]
8. Khatibi, S.A.; Hamidi, S.; Siahi-Shadbad, M.R. Current trends in sample preparation by solid-phase extraction techniques for the determination of antibiotic residues in foodstuffs: A review. *Crit. Rev. Food Sci. Nutr.* **2021**, *61*, 3361–3382. [CrossRef] [PubMed]
9. Chen, D.; Yu, J.; Tao, Y.; Pan, Y.; Xie, S.; Huang, L.; Peng, D.; Wang, X.; Wang, Y.; Liu, Z.; et al. Qualitative screening of veterinary anti-microbial agents in tissues, milk, and eggs of food-producing animals using liquid chromatography coupled with tandem mass spectrometry. *J. Chromatogr. B Anal. Technol. Biomed. Life Sci.* **2016**, *1017–1018*, 82–88. [CrossRef]
10. Bohm, D.A.; Stachel, C.S.; Gowik, P. Multi-method for the determination of antibiotics of different substance groups in milk and validation in accordance with Commission Decision 2002/657/EC. *J. Chromatogr. A* **2009**, *1216*, 8217–8223. [CrossRef]
11. Wang, J.; Leung, D. Analyses of macrolide antibiotic residues in eggs, raw milk, and honey using both ultra-performance liquid chromatography/quadrupole time-of-flight mass spectrometry and high-performance liquid chromatography/tandem mass spectrometry. *Rapid Commun. Mass Spectrom.* **2007**, *21*, 3213–3222. [CrossRef] [PubMed]
12. Wang, J.; Leung, D.; Butterworth, F. Determination of Five Macrolide Antibiotic Residues in Eggs Using Liquid Chromatography/Electrospray Ionization Tandem Mass Spectrometry. *J. Agric. Food Chem.* **2005**, *53*, 1857–1865. [CrossRef] [PubMed]
13. Garrido Frenich, A.; del Aguilera-Luiz, M.M.; Martínez Vidal, J.L.; Romero-González, R. Comparison of several extraction techniques for multiclass analysis of veterinary drugs in eggs using ultra-high pressure liquid chromatography-tandem mass spectrometry. *Anal. Chim. Acta* **2010**, *661*, 150–160. [CrossRef] [PubMed]
14. González-Gómez, L.; Morante-Zarcero, S.; Pérez-Quintanilla, D.; González, G.P.; Garcinuño, R.M.; Hernando, P.F.; Sierra, I. Fibreglass membrane chemically modified with amino-functionalised SBA-15 and its application in solid-phase extraction to determine macrolide antibiotics in eggs. *Microchem. J.* **2024**, *205*, 111232–111245. [CrossRef]
15. Leal, C.; Codony, R.; Compañó, R.; Granados, M.; Prat, M.D. Determination of macrolide antibiotics by liquid chromatography. *J. Chromatogr. A* **2001**, *910*, 285–290. [CrossRef]
16. López-Lorente, Á.I.; Pena-Pereira, F.; Pedersen-Bjergaard, S.; Zuin, V.G.; Ozkan, S.A.; Psillakis, E. The ten principles of green sample preparation. *TrAC Trends Anal. Chem.* **2022**, *148*, 116530. [CrossRef]
17. Sierra, I.; Morante-Zarcero, S. New Advances in Food Sample Preparation with Nanomaterials for Organic Contaminants Analysis by Liquid Chromatography. In *Nanomaterials in Chromatography*; Elsevier: Amsterdam, The Netherlands, 2018; pp. 118–154. ISBN 9780128127926.
18. Vasapollo, G.; Del Sole, R.; Mergola, L.; Lazzoi, M.R.; Scardino, A.; Scorrano, S.; Mele, G. Molecularly imprinted polymers: Present and future prospective. *Int. J. Mol. Sci.* **2011**, *12*, 5908–5945. [CrossRef]
19. Turiel, E.; Martín-Esteban, A. Molecularly imprinted polymers for sample preparation: A review. *Anal. Chim. Acta* **2010**, *668*, 87–99. [CrossRef]
20. He, H.; Gu, X.; Shi, L.; Hong, J.; Zhang, H.; Gao, Y.; Du, S.; Chen, L. Molecularly imprinted polymers based on SBA-15 for selective solid-phase extraction of baicalein from plasma samples. *Anal. Bioanal. Chem.* **2015**, *407*, 509–519. [CrossRef]
21. Yang, F.; Hu, D.; Dong, X. Molecularly Imprinted Mesoporous SBA-15 Synthesized by Surface-Initiated Atom Transfer Radical Polymerization for Bisphenol A Recognition. *Chromatographia* **2015**, *78*, 45–54. [CrossRef]
22. Wang, H.; Liu, Y.; Yao, S.; Zhu, P. Selective recognization of dicyandiamide in bovine milk by mesoporous silica SBA-15 supported dicyandiamide imprinted polymer based on surface molecularly imprinting technique. *Food Chem.* **2018**, *240*, 1262–1267. [CrossRef]
23. Costa, J.A.S.; De Jesus, R.A.; Santos, D.O.; Neris, J.B.; Figueiredo, R.T.; Paranhos, C.M. Synthesis, functionalization, and environmental application of silica-based mesoporous materials of the M41S and SBA-n families: A review. *J. Environ. Chem. Eng.* **2021**, *9*, 105259. [CrossRef]
24. Naik, B.; Ghosh, N. A Review on Chemical Methodologies for Preparation of Mesoporous Silica and Alumina Based Materials. *Recent Pat. Nanotechnol.* **2009**, *3*, 213–224. [CrossRef]
25. Kresge, C.T.; Leonowicz, M.E.; Roth, W.J.; Vartuli, J.C.; Beck, J.S. Ordered mesoporous molecular sieves synthesized by a liquid-crystal template mechanism. *Nature* **1992**, *359*, 710–712. [CrossRef]
26. Zhao, D.; Feng, J.; Huo, Q.; Melosh, N.; Fredrickson, G.H.; Chmelka, B.F.; Stucky, G.D. Triblock Copolymer Syntheses of Mesoporous Silica with Periodic 50 to 300 Angstrom Pores. *Science* **1998**, *279*, 548–552. [CrossRef] [PubMed]
27. Wang, D.; Chen, X.; Feng, J.; Sun, M. Recent advances of ordered mesoporous silica materials for solid-phase extraction. *J. Chromatogr. A* **2022**, *1675*, 463157. [CrossRef]
28. Mehdinia, A.; Ahmadifar, M.; Aziz-Zanjani, M.O.; Jabbari, A.; Hashtroudi, M.S. Selective adsorption of 2,4-dinitrophenol on molecularly imprinted nanocomposites of mesoporous silica SBA-15/polyaniline. *Analyst* **2012**, *137*, 4368–4374. [CrossRef]
29. Zhao, D.; Huo, Q.; Feng, J.; Chmelka, B.F.; Stucky, G.D. Nonionic triblock and star diblock copolymer and oligomeric sufactant syntheses of highly ordered, hydrothermally stable, mesoporous silica structures. *J. Am. Chem. Soc.* **1998**, *120*, 6024–6036. [CrossRef]

30. Casado, N.; Morante-Zarcero, S.; Sierra, I. Miniaturized Analytical Strategy Based on µ-SPEed for Monitoring the Occurrence of Pyrrolizidine and Tropane Alkaloids in Honey. *J. Agric. Food Chem.* **2024**, *72*, 819–832. [CrossRef]
31. García Mayor, M.A.; Paniagua González, G.; Garcinuño Martínez, R.M.; Fernández Hernando, P.; Durand Alegría, J.S. Synthesis and characterization of a molecularly imprinted polymer for the determination of spiramycin in sheep milk. *Food Chem.* **2017**, *221*, 721–728. [CrossRef]

Disclaimer/Publisher's Note: The statements, opinions and data contained in all publications are solely those of the individual author(s) and contributor(s) and not of MDPI and/or the editor(s). MDPI and/or the editor(s) disclaim responsibility for any injury to people or property resulting from any ideas, methods, instructions or products referred to in the content.